

# **Effect of Rheology on Afterslip and Viscoelastic Patterns Following the 2010 Mw 8.8 Maule, Chile, Earthquake**

**Carlos Peña** <sup>1, 2</sup>, Oliver Heidbach<sup>1</sup>, Marcos Moreno<sup>3</sup>, Jonathan Bedford<sup>1</sup>, Moritz Ziegler<sup>1</sup>, Andrés Tassara<sup>4, 5</sup> and Onno Oncken<sup>1, 2</sup>

<sup>1</sup> Helmholtz Centre Potsdam, GFZ German Research Centre for Geosciences, Potsdam, Germany

<sup>2</sup> Freie Universität Berlin, Berlin, Germany

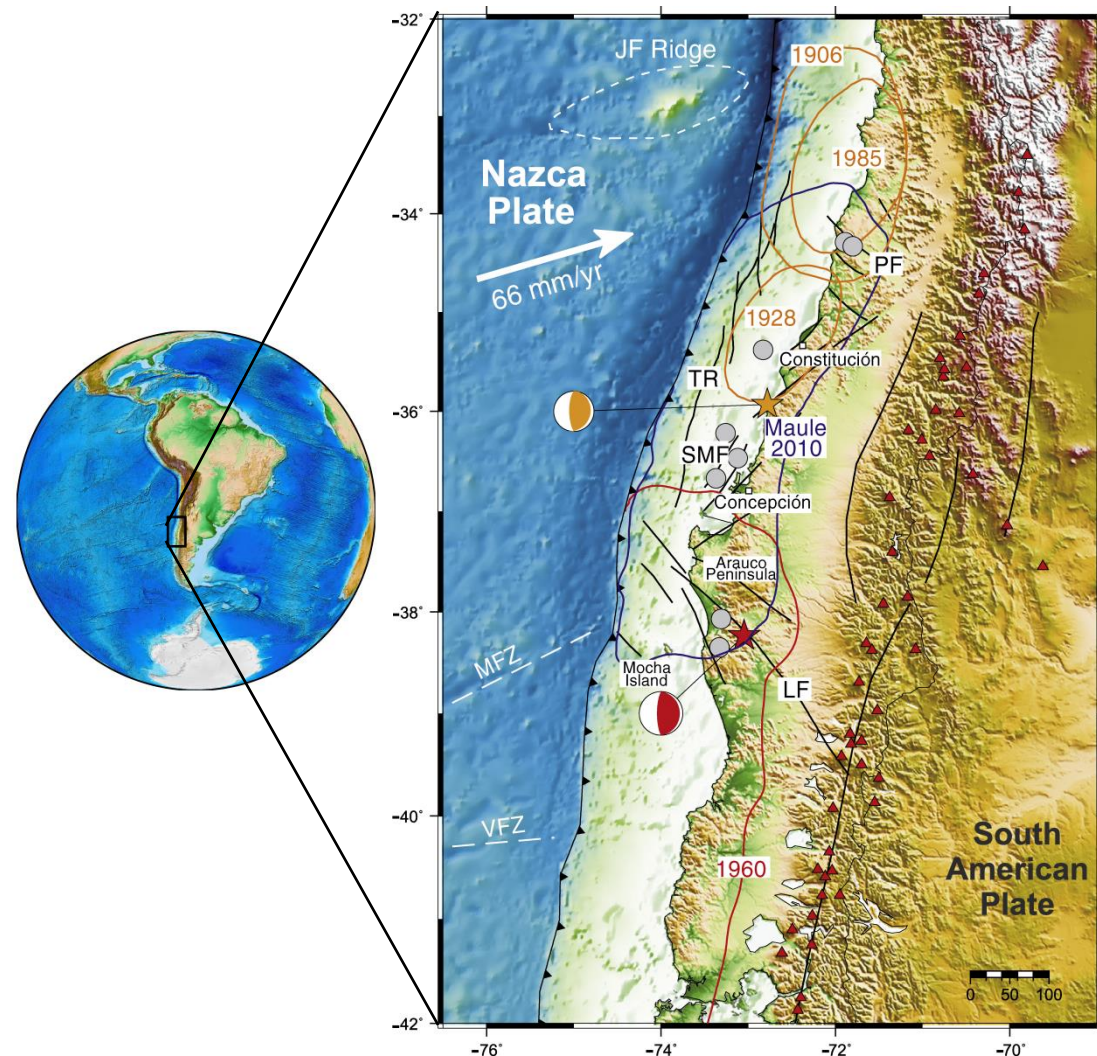
<sup>3</sup> Departamento de Geofísica, Universidad de Concepción, Chile

<sup>4</sup> Departamento de Ciencias de la Tierra, Universidad de Concepción, Chile

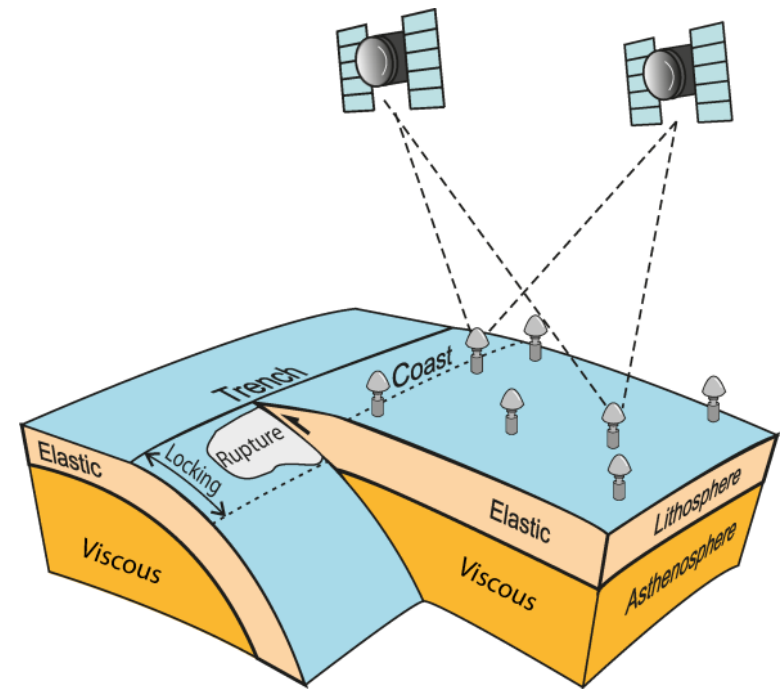
<sup>5</sup> Millennium Nucleus CYCLO “The Seismic Cycle along Subduction Zones”

Contact: [carlosp@gfz-potsdam.de](mailto:carlosp@gfz-potsdam.de)

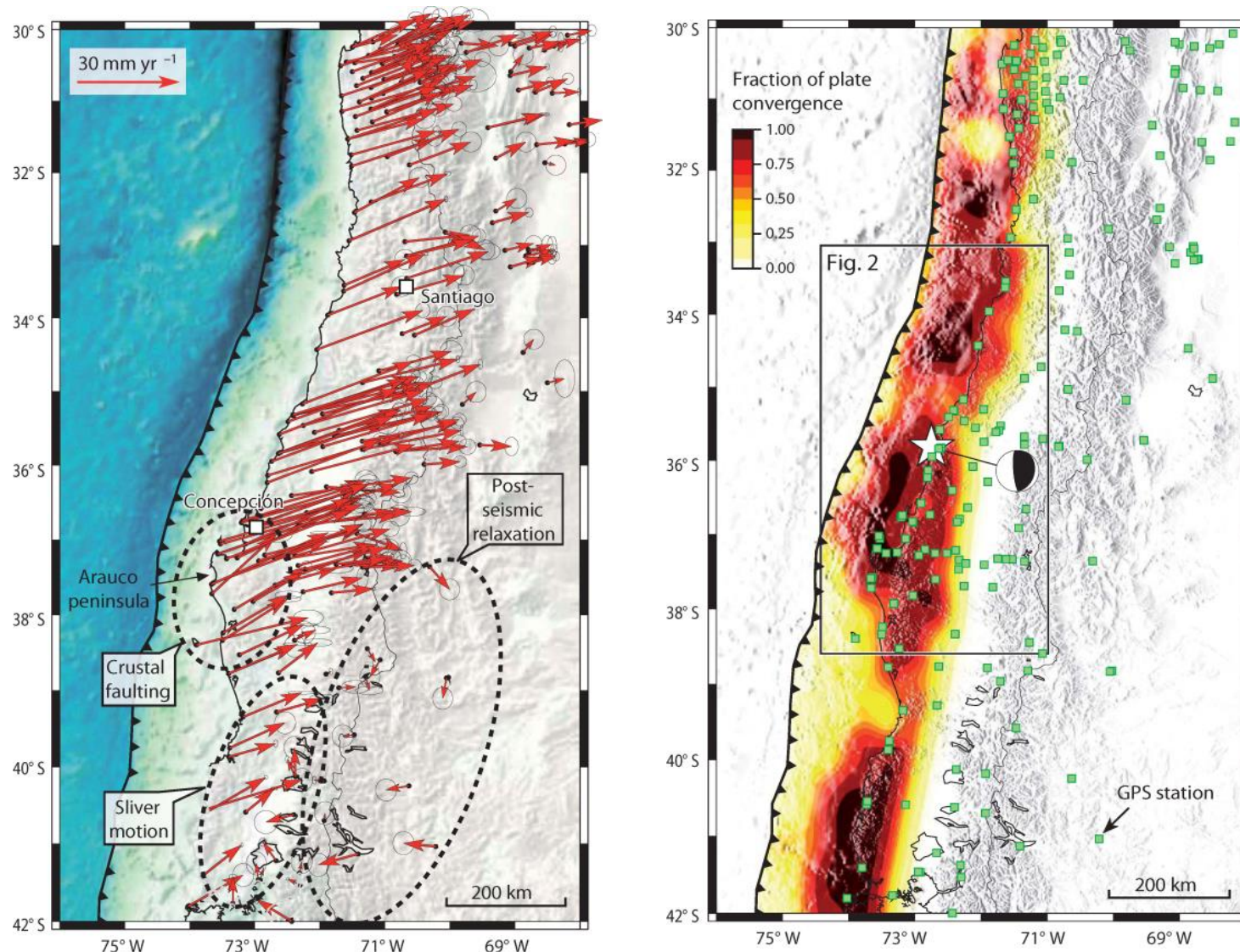
# The seismic cycle constrained by GPS observations



GPS observations network

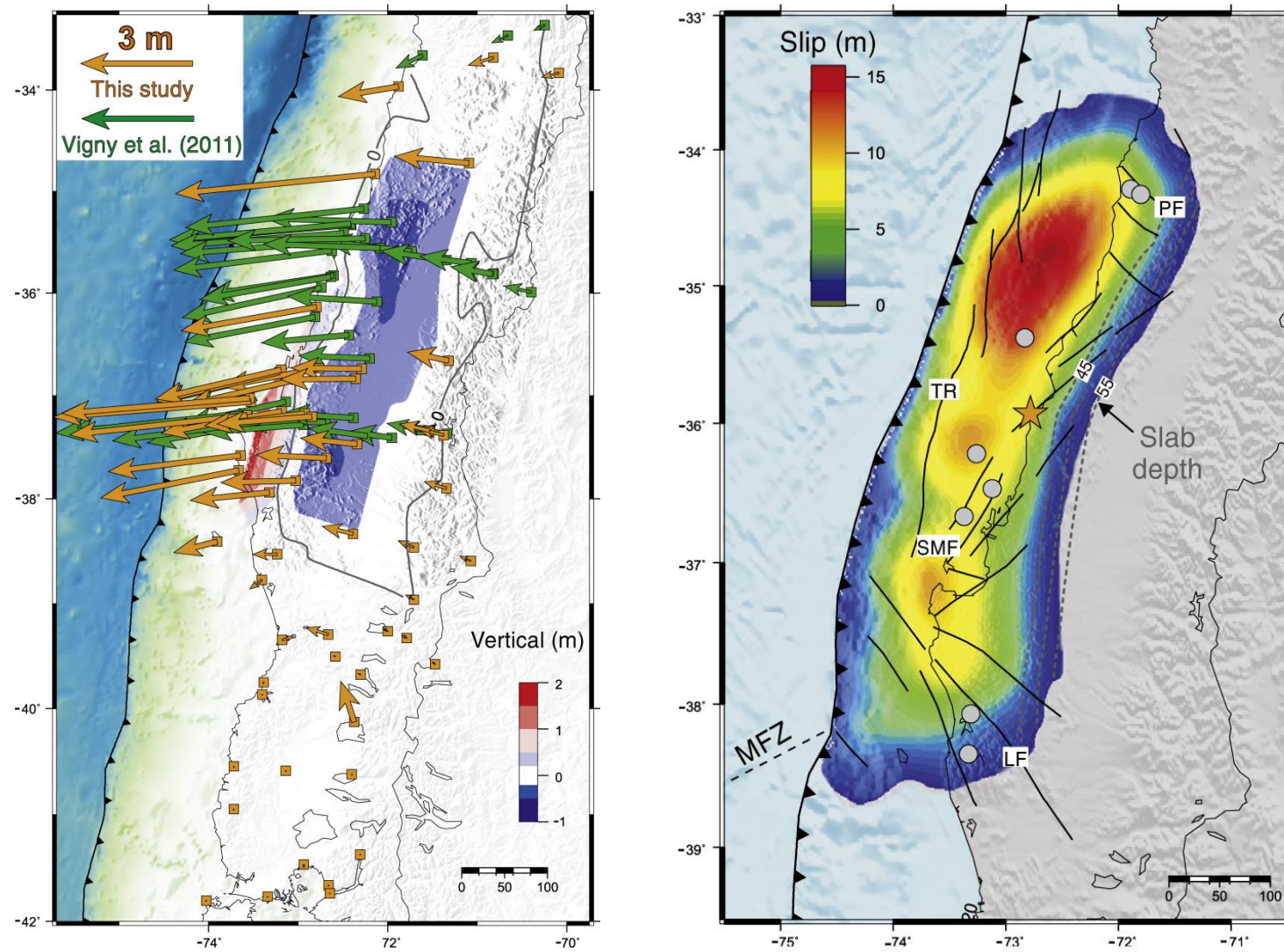


# Interseismic GPS observations



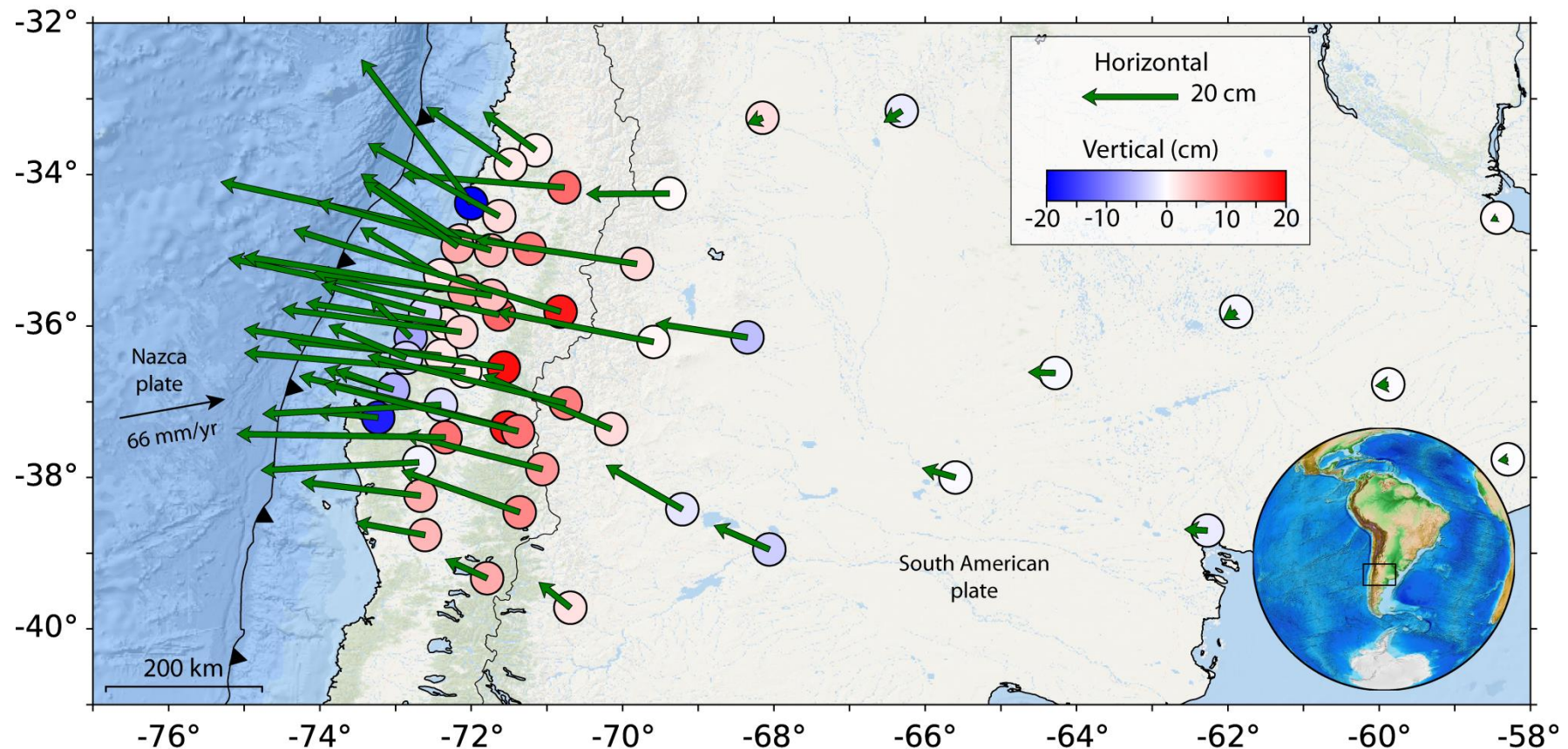
Modified from Moreno et al. (2010)

# Coseismic GPS observations



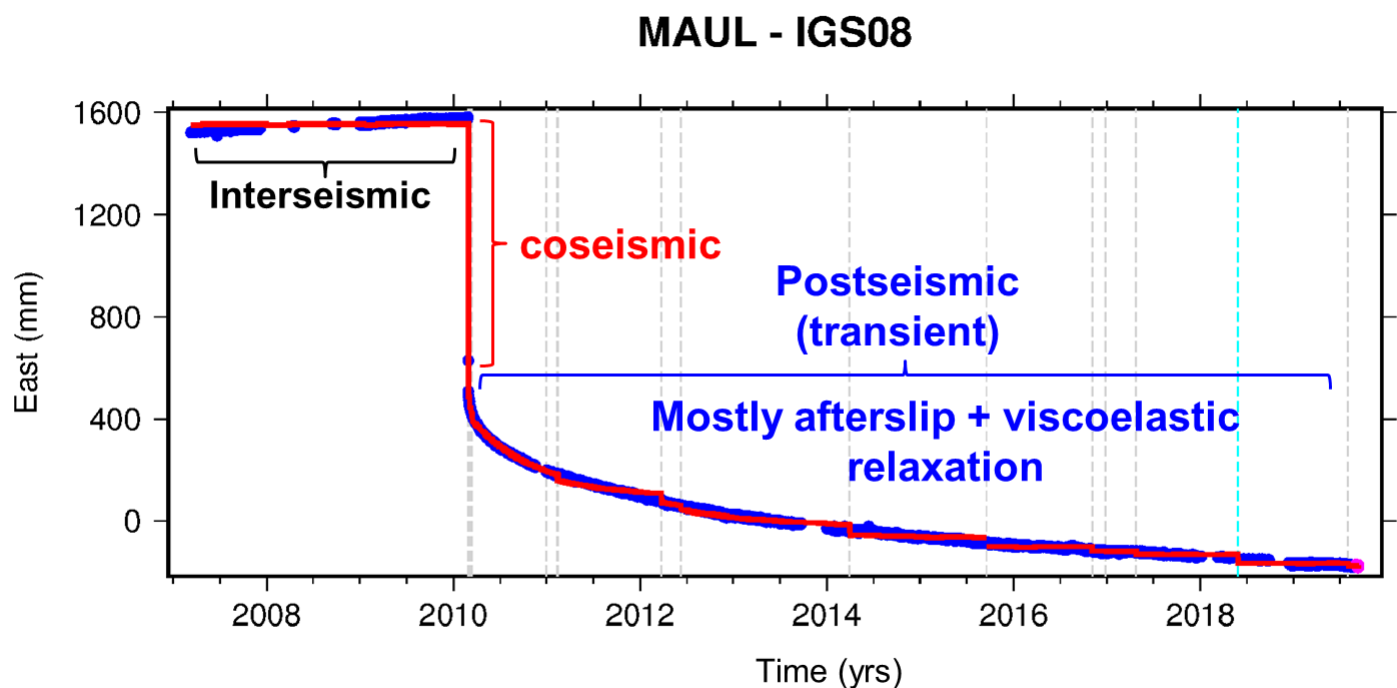
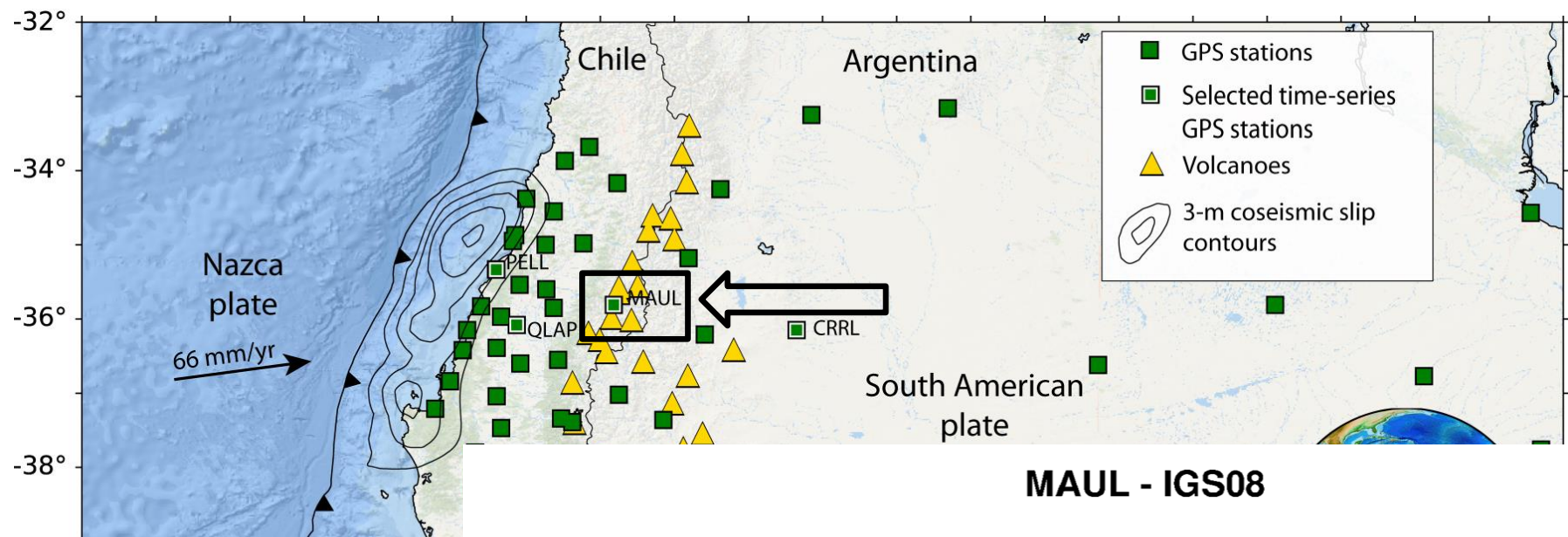
Modified from Moreno et al. (2012)

# Postseismic GPS Observations

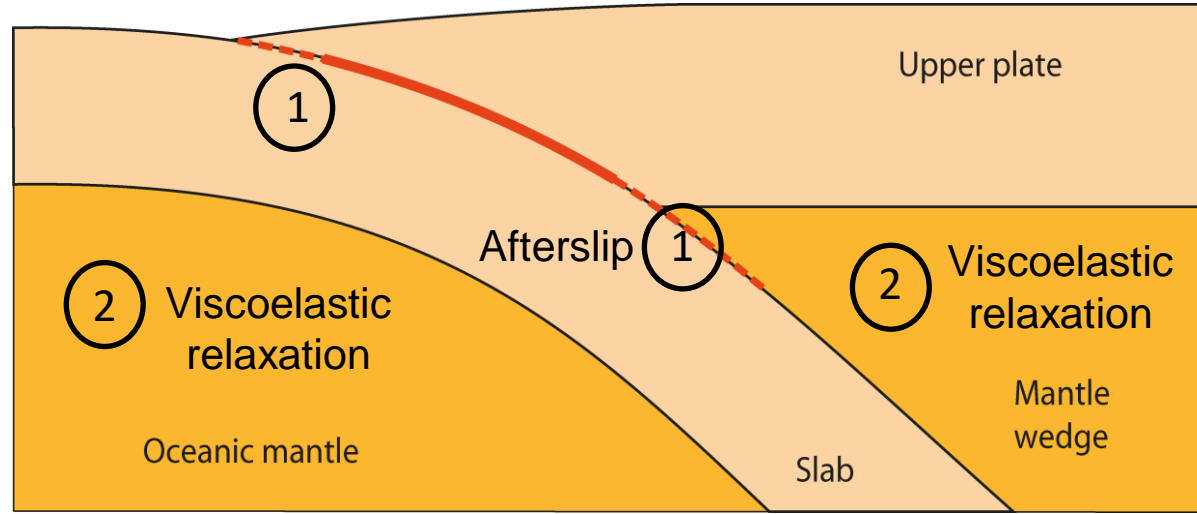


- Six years of cumulative postseismic displacements (Li et al., 2017)
- Aftershock and/or jumps, and secular were removed
- Stable South American frame

# Postseismic GPS Observations



# Afterslip inversions need a rheology model

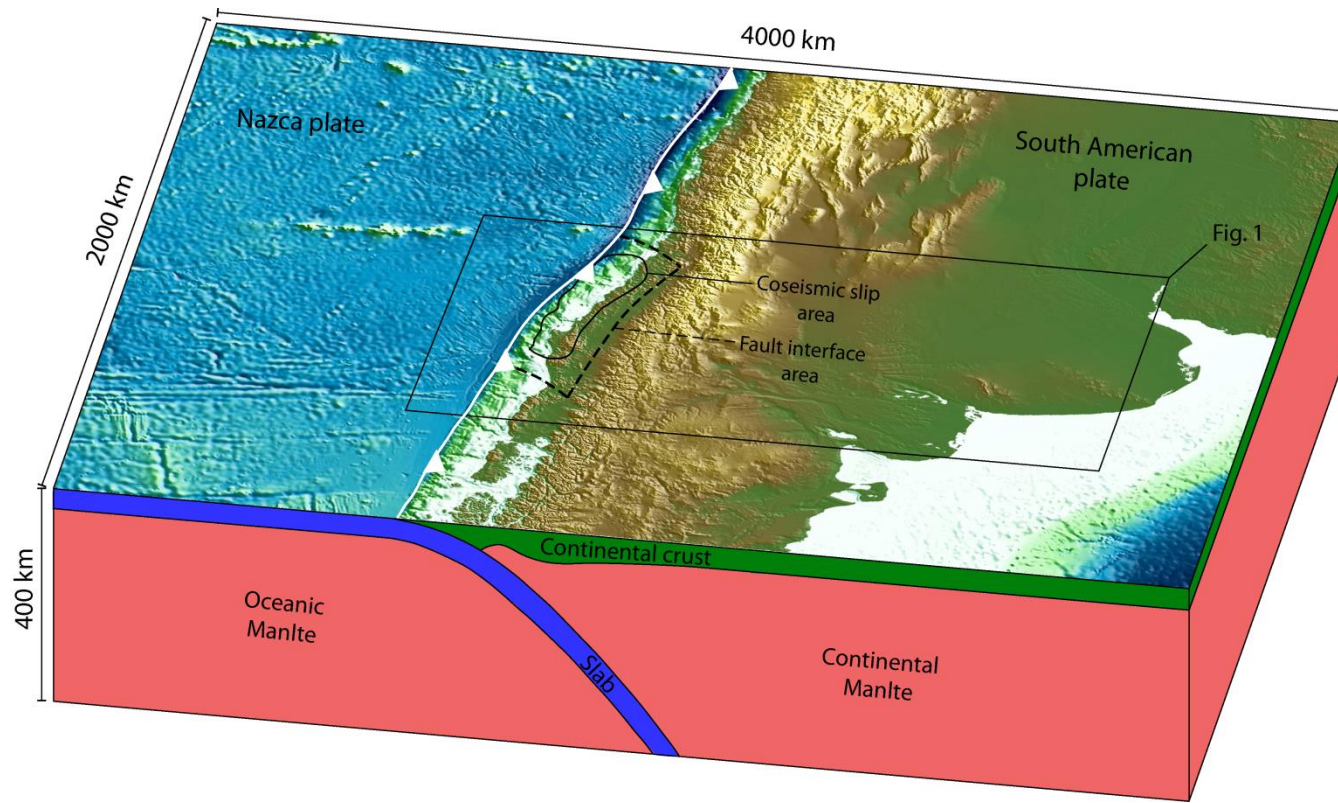


Modified from Wang et al. (2012)

**How different can afterslip distribution at the fault interface result from the choice of rheology?**

**Note:** the following slides contain figures (model setup, workflow, results, and afterslip-aftershock correlation) modified from the original study of C. Peña et al. (2020), EPSL (in press),  
<https://doi.org/10.1016/j.epsl.2020.116292>

# 3D-FEM Model Setup



## Discontinuities (geometry)

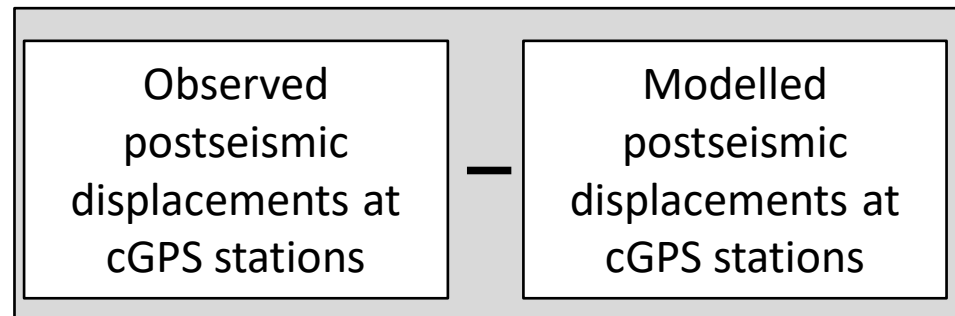
- Slab (Hayes et al., 2012)
- Moho (Tassara et al., 2006)

## Boundary and initial conditions

- Coseismic slip model (Moreno et al., 2012)
- Temperature field (Völker et al., 2011)

# Afterslip Inversion Workflow

## Step 1: Viscoelastic forward modelling



## Step 2: Inversion

- Least square
- Non-negative rake
- Smoothing laplacian

## Result

Afterslip distribution

Input

$$\dot{\varepsilon} = A\sigma^n \exp\left(\frac{-Q}{RT}\right) \quad (1)$$

Power-law rheology  
(Dislocation creep)

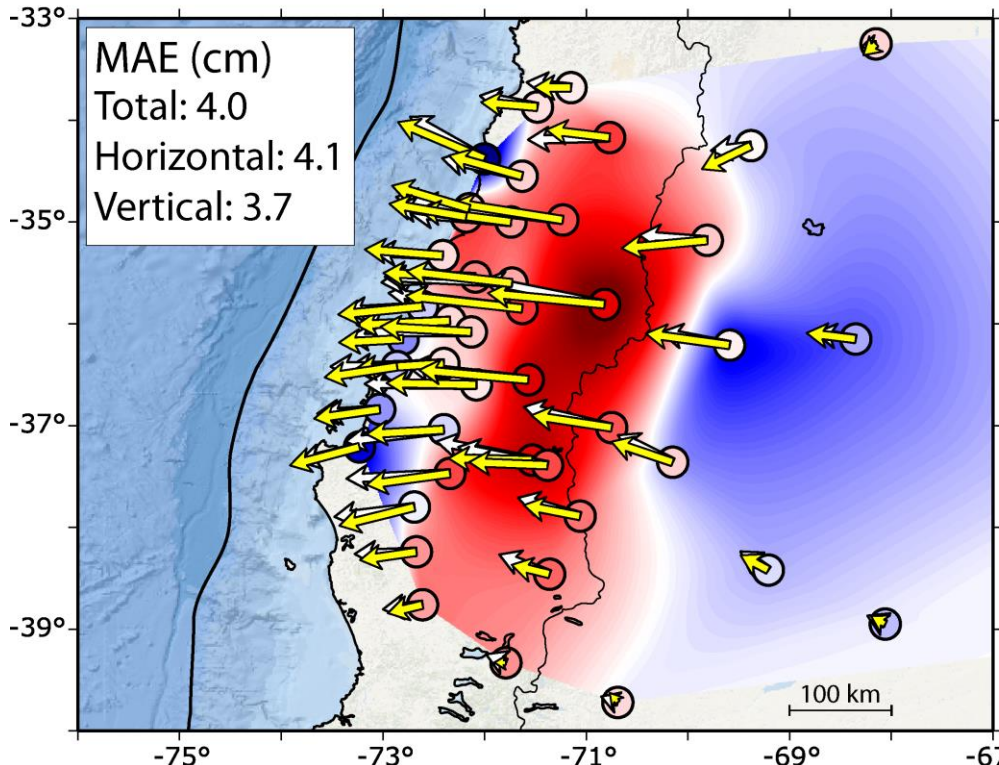
$$\dot{\varepsilon} = \frac{\sigma}{2\eta} \quad (2)$$

Linear rheology  
( $\eta = \text{constant}$ )

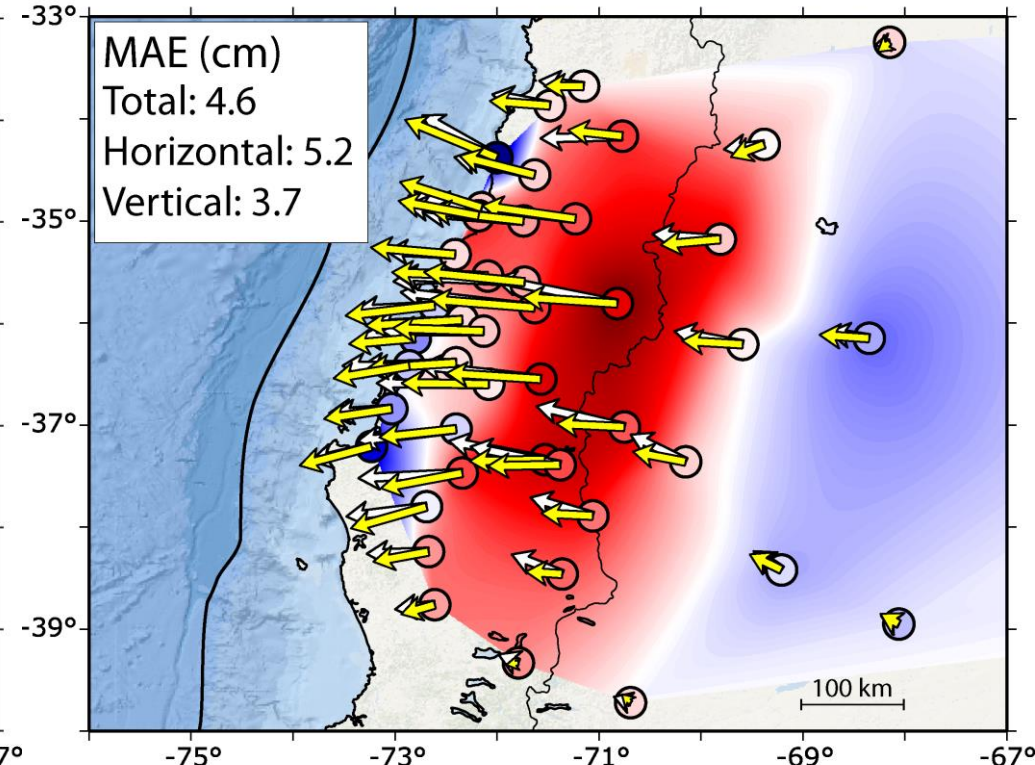
- $\dot{\varepsilon}$  creep strain rate
- $A$  material constant
- $\sigma$  differential stress
- $\eta$  effective viscosity
- $Q$  activation enthalpy
- $R$  gas constant
- $T$  absolute temperature  
(from Völker et al., 2011)

# Results: Surface Displacements

Power-law rheology, weak crust (quartzite)



Power-law rheology, strong crust (diabase)

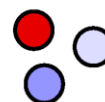
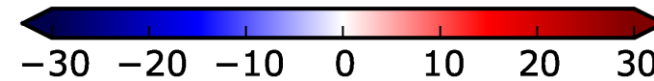


Power-law simulations have same creep parameters for: Cont. mantle: Olivine 0.1 wt.% water, Slab: Diabase, Ocea. mantle: Olivine 0.005 wt.% water

Horizontal displacement

50 cm  
↔ Observed  
→ Modelled  
(Afterslip + viscoelastic)

Vertical displacement (cm)

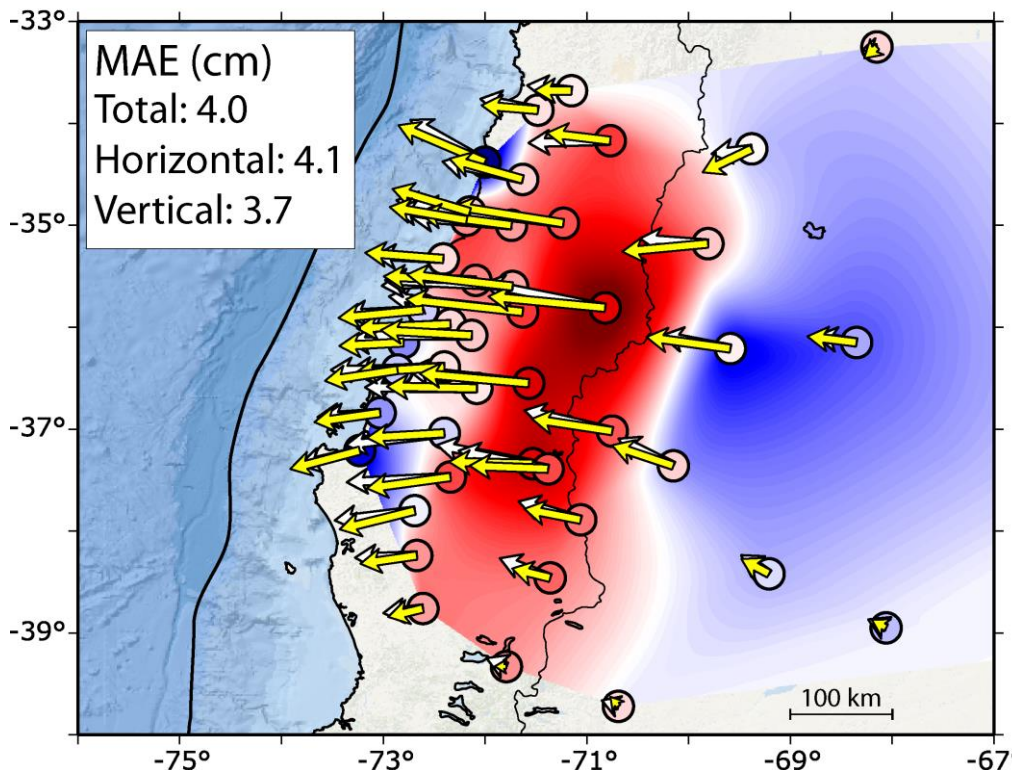


Observed

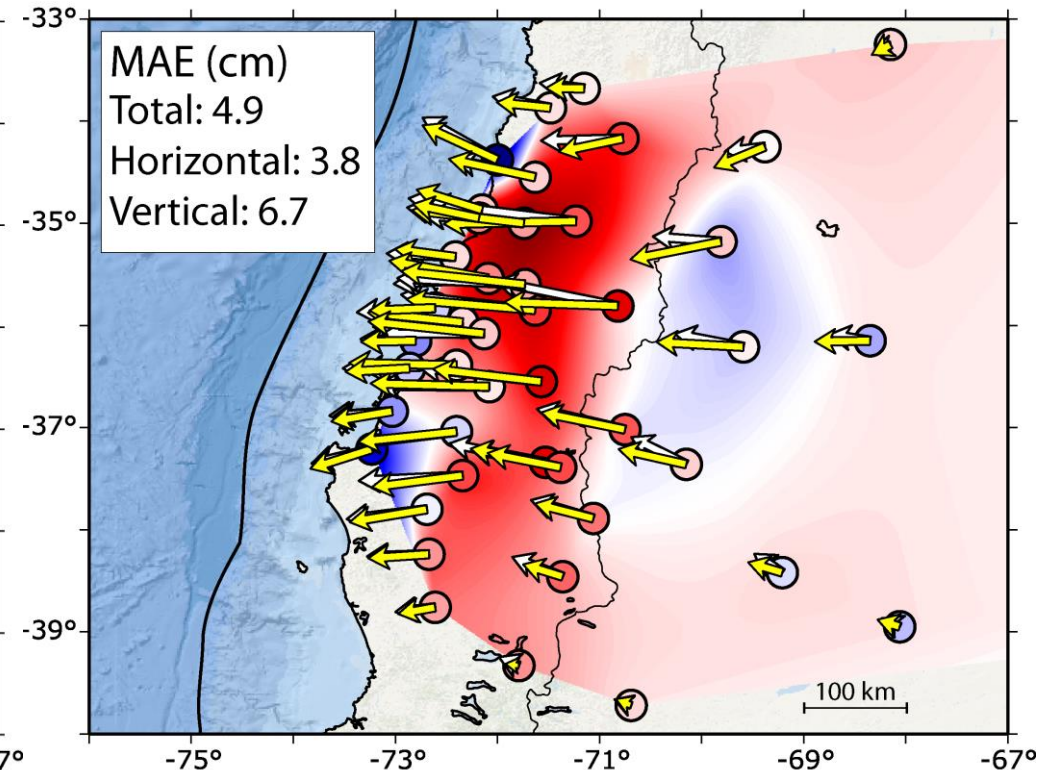
Color-coded: Modelled (Afterslip + viscoelastic)

# Results: Surface Displacements

Power-law rheology, weak crust (quartzite)



Linear rheology, elastic crust

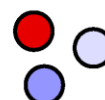


Linear rheology simulation: Mantle: linear viscosity, slab: elastic

Horizontal displacement

50 cm  
↔ Observed  
↔ Modelled  
(Afterslip + viscoelastic)

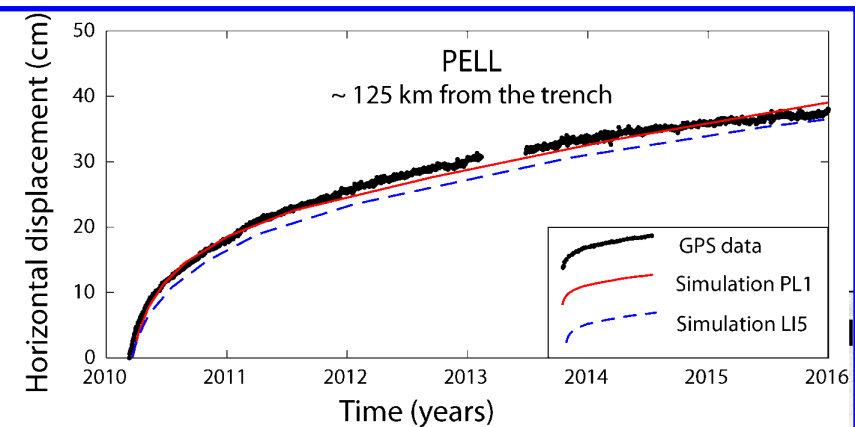
Vertical displacement (cm)



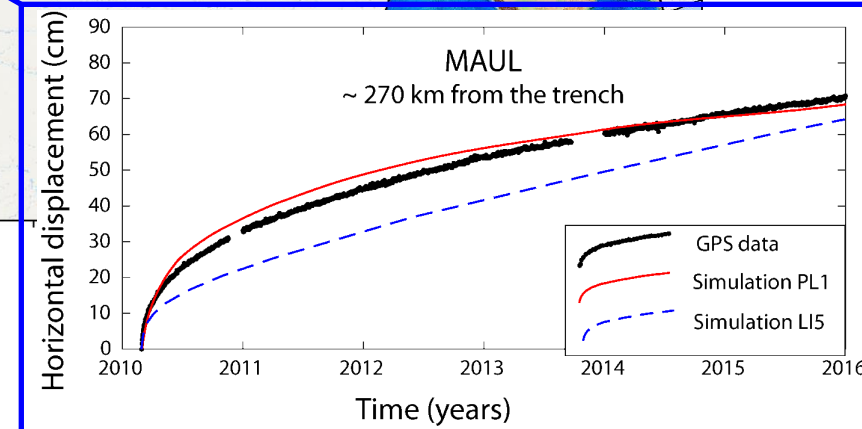
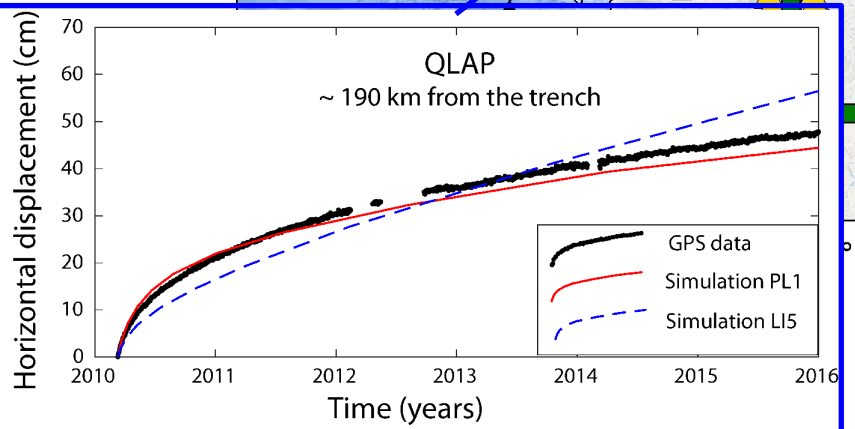
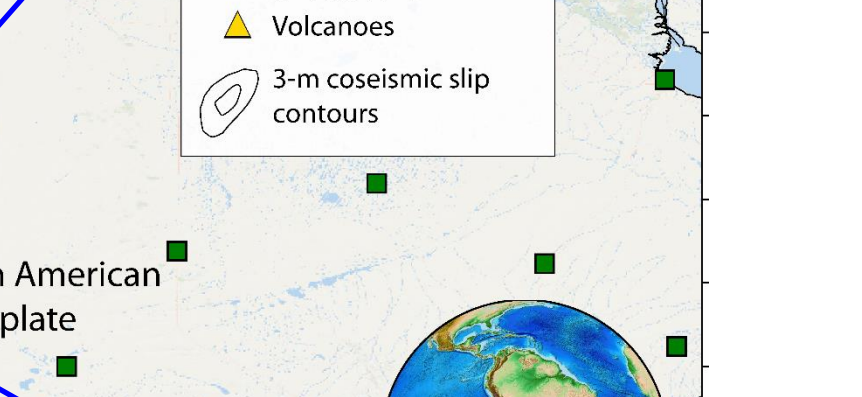
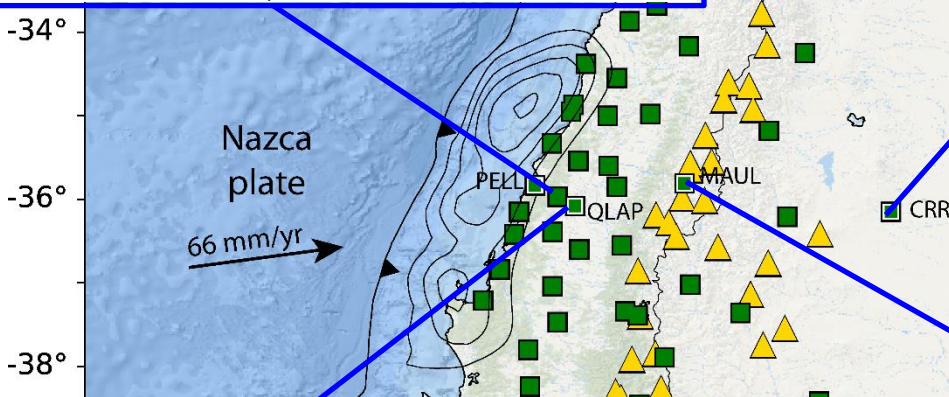
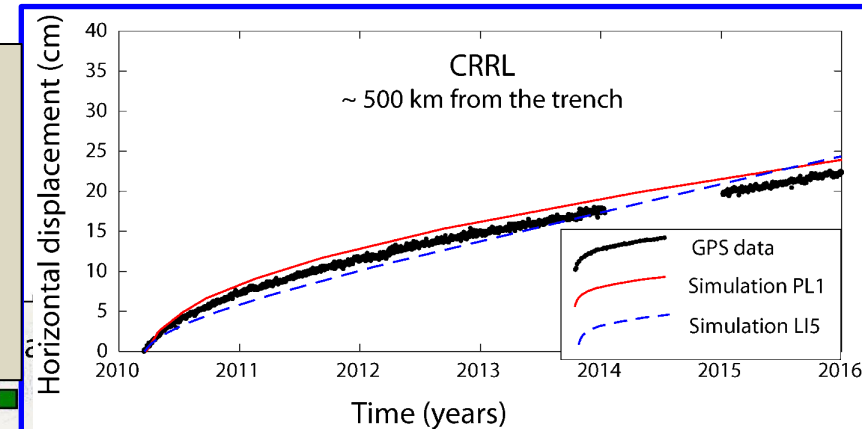
Observed

Color-coded: Modelled (Afterslip + viscoelastic)

# Results: Linear vs Power-law time series

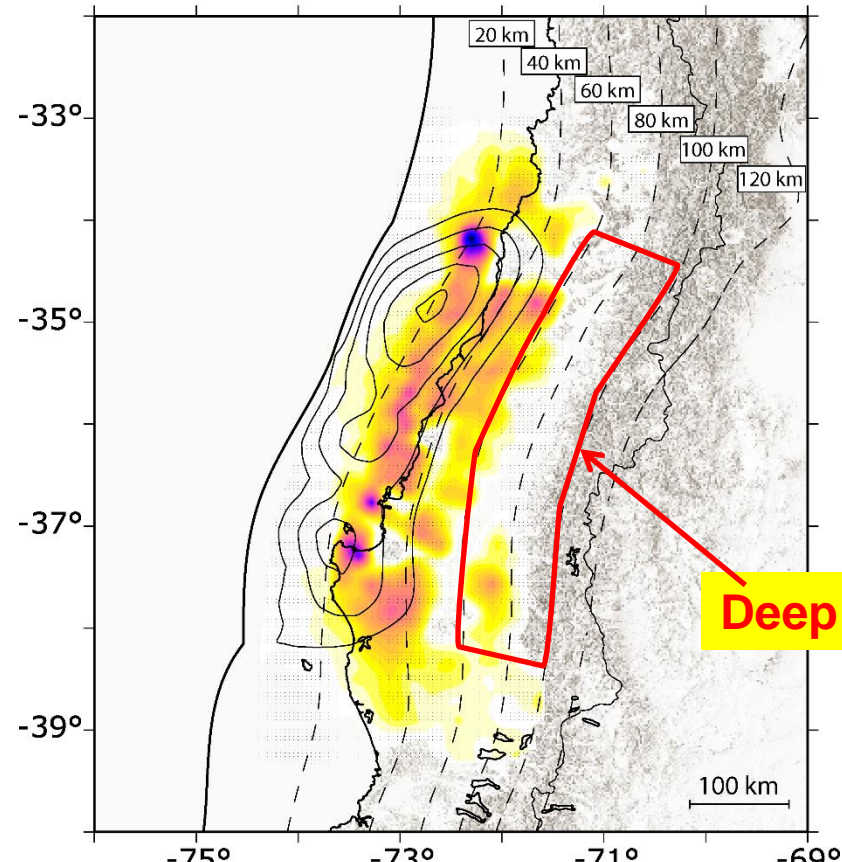


**PL1:** Power-law rheology, weak crust (red solid line)  
**LI5:** Linear rheology, elastic crust (blue dashed line)



# Results: Afterslip Distributions

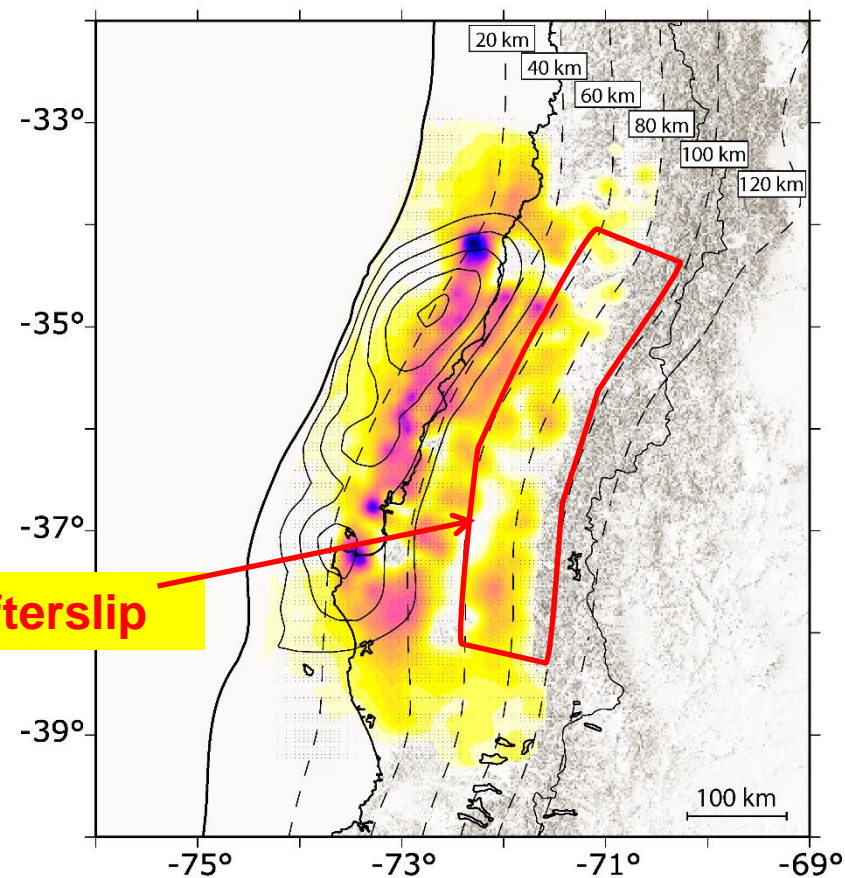
Power-law rheology, weak crust (quartzite)



Afterslip (m)



Power-law rheology, strong crust (diabase)



3-m coseismic slip contours

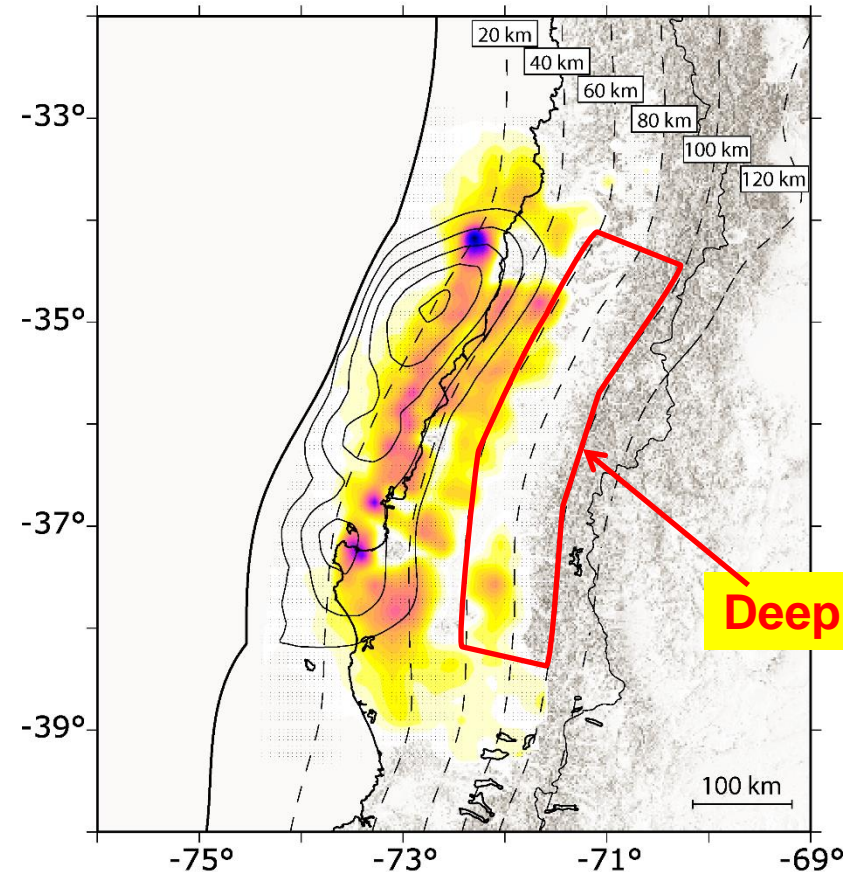


Slab surface depth

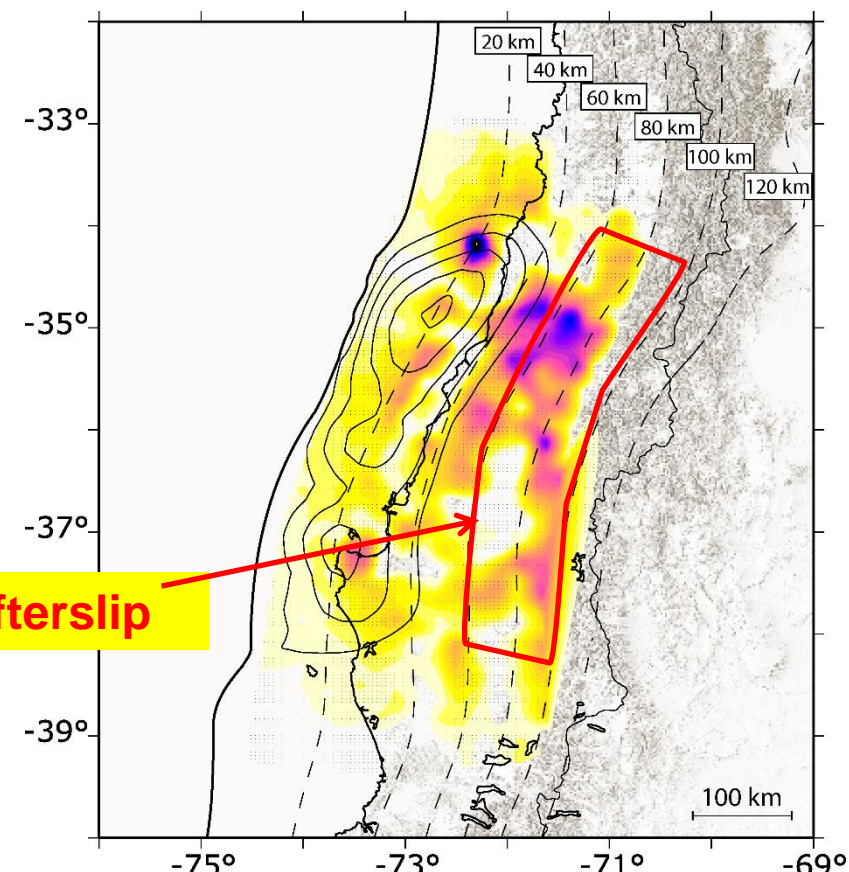


# Results: Afterslip Distributions

Power-law rheology, weak crust (quartzite)



Linear rheology, elastic crust



Afterslip (m)



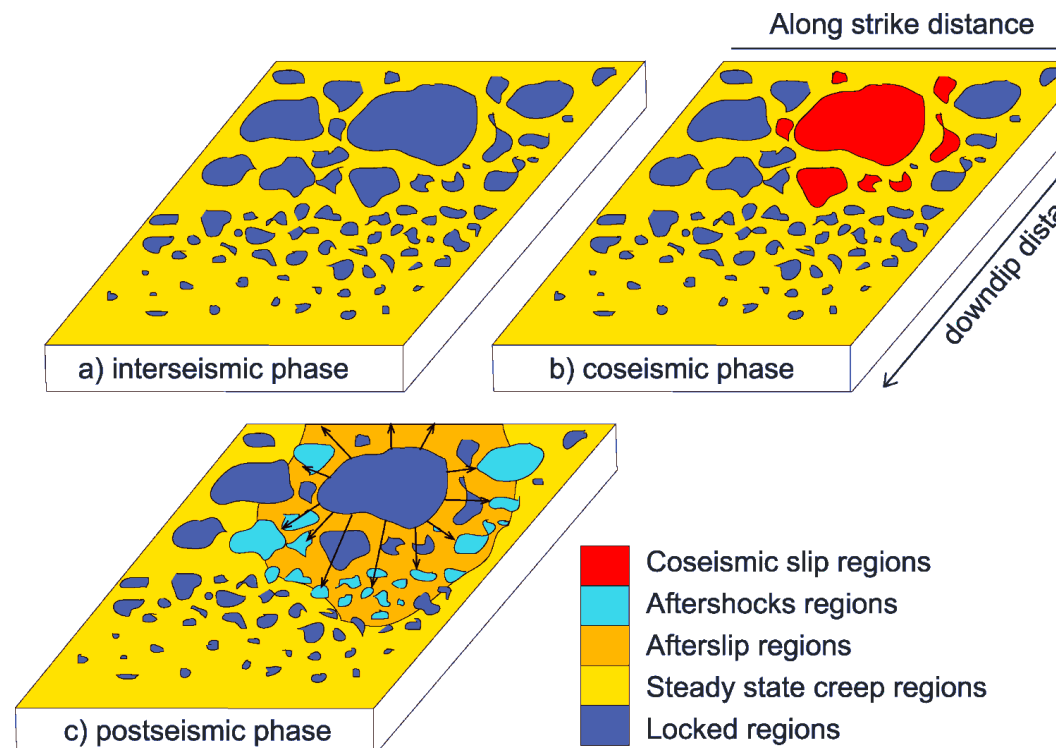
3-m coseismic slip contours



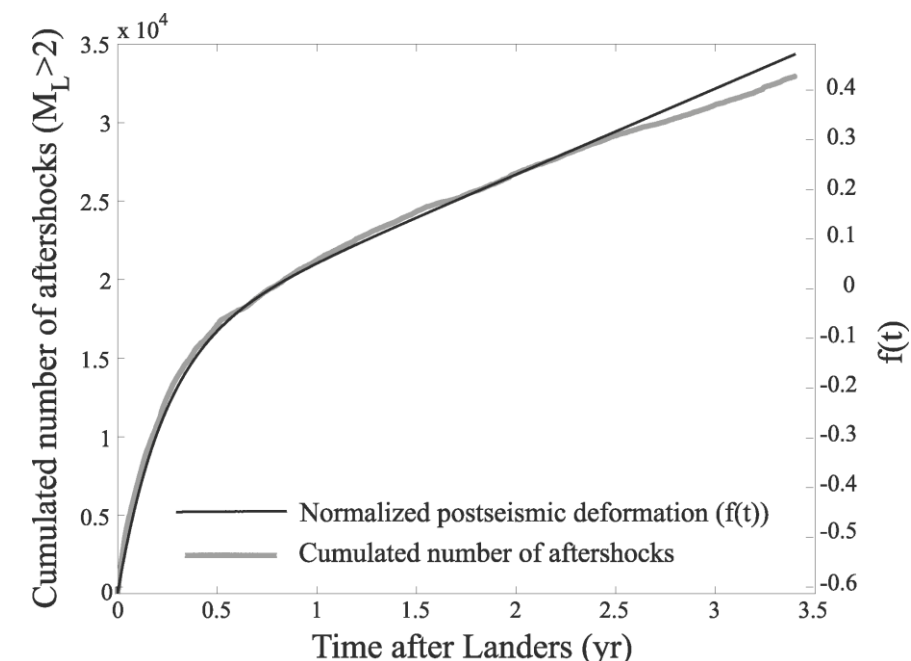
Slab surface depth



# Afterslip generally drives aftershocks



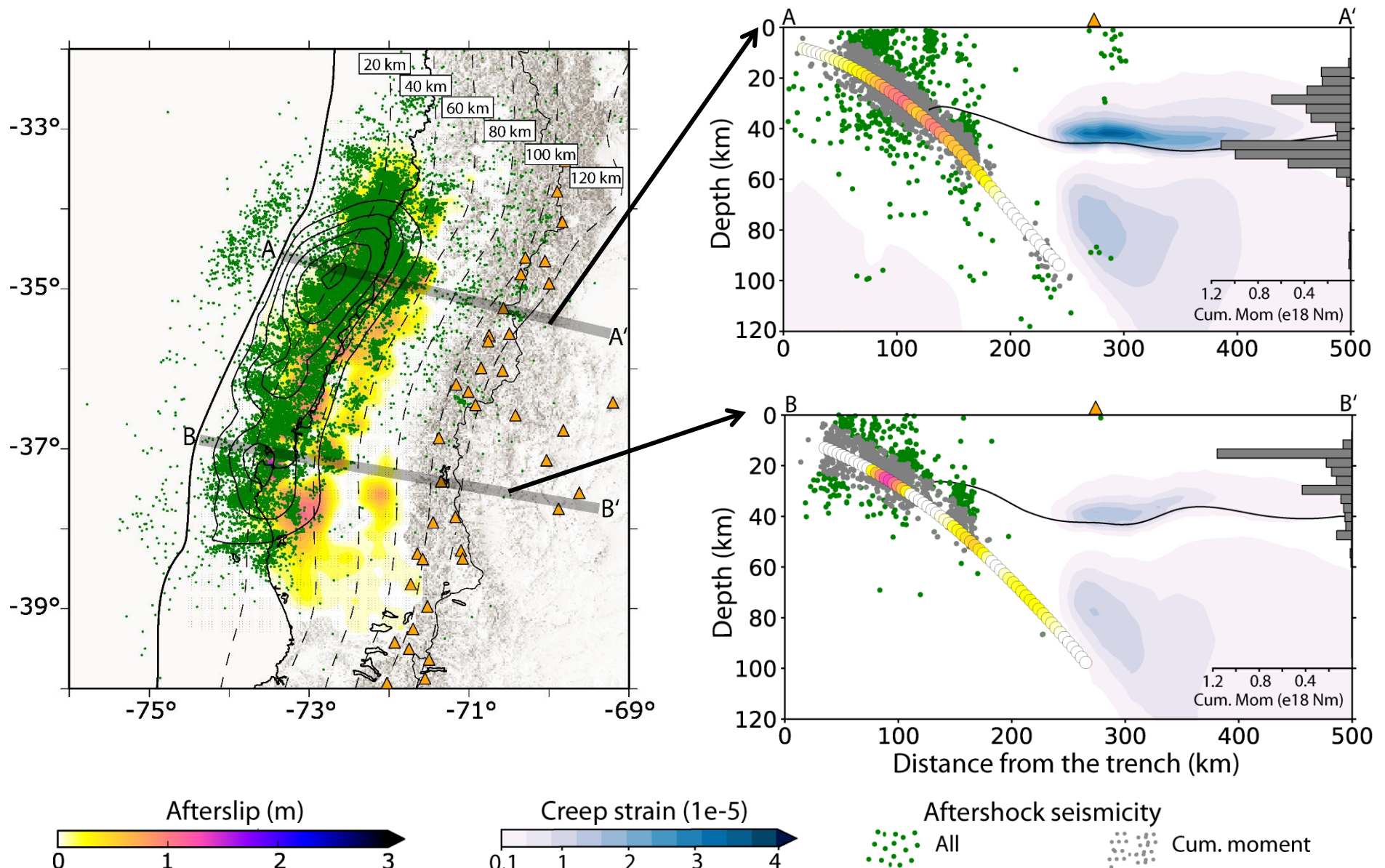
Perfettini et al. (2018)



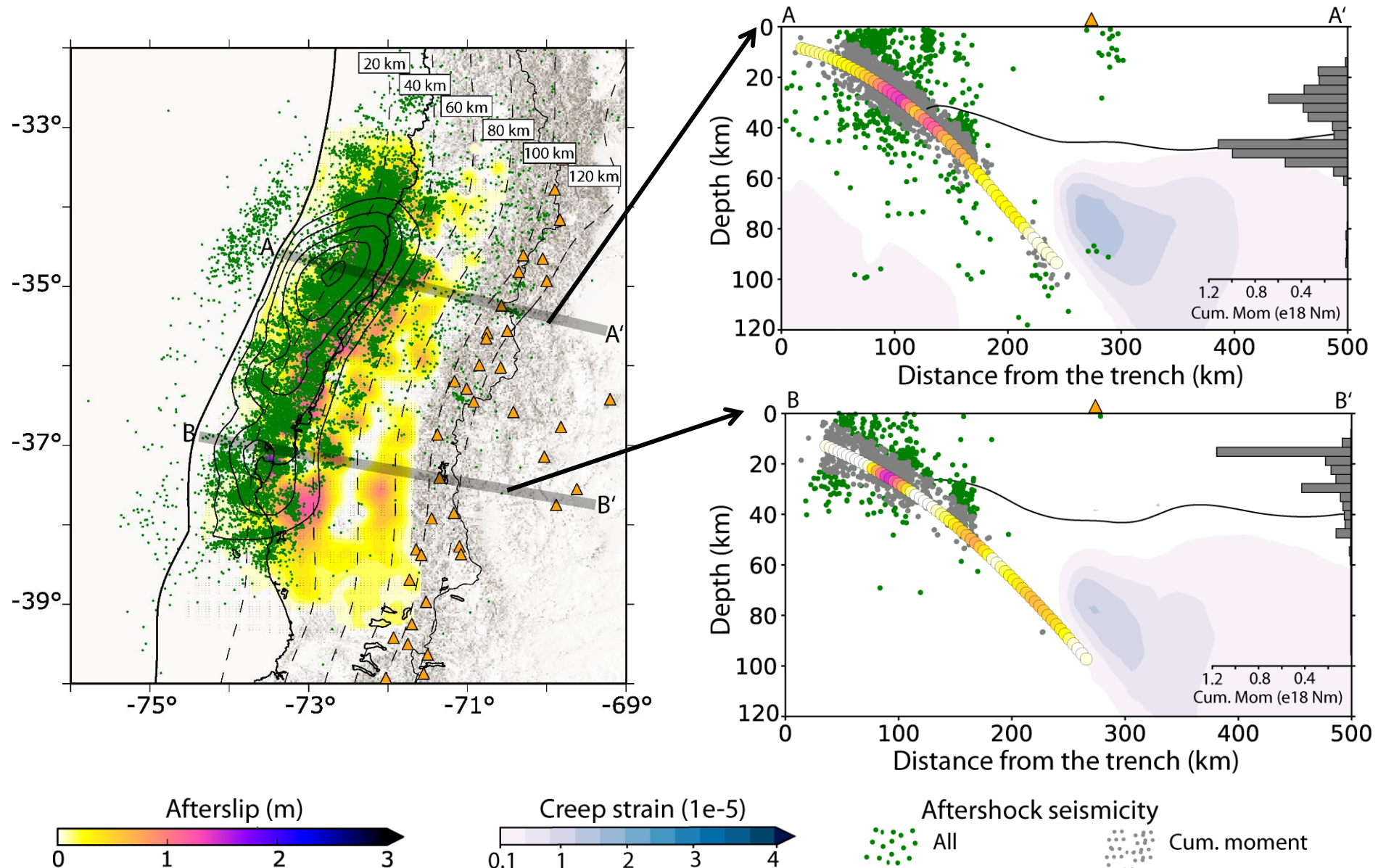
Perfettini and Avouac (2007)

**Further reading:** Agurto et al. (2019), Avouac (2005), Bedford et al. (2016), Hsu et al. (2006), Peng and Zhao (2009), Lange et al (2014), Kato (2007)

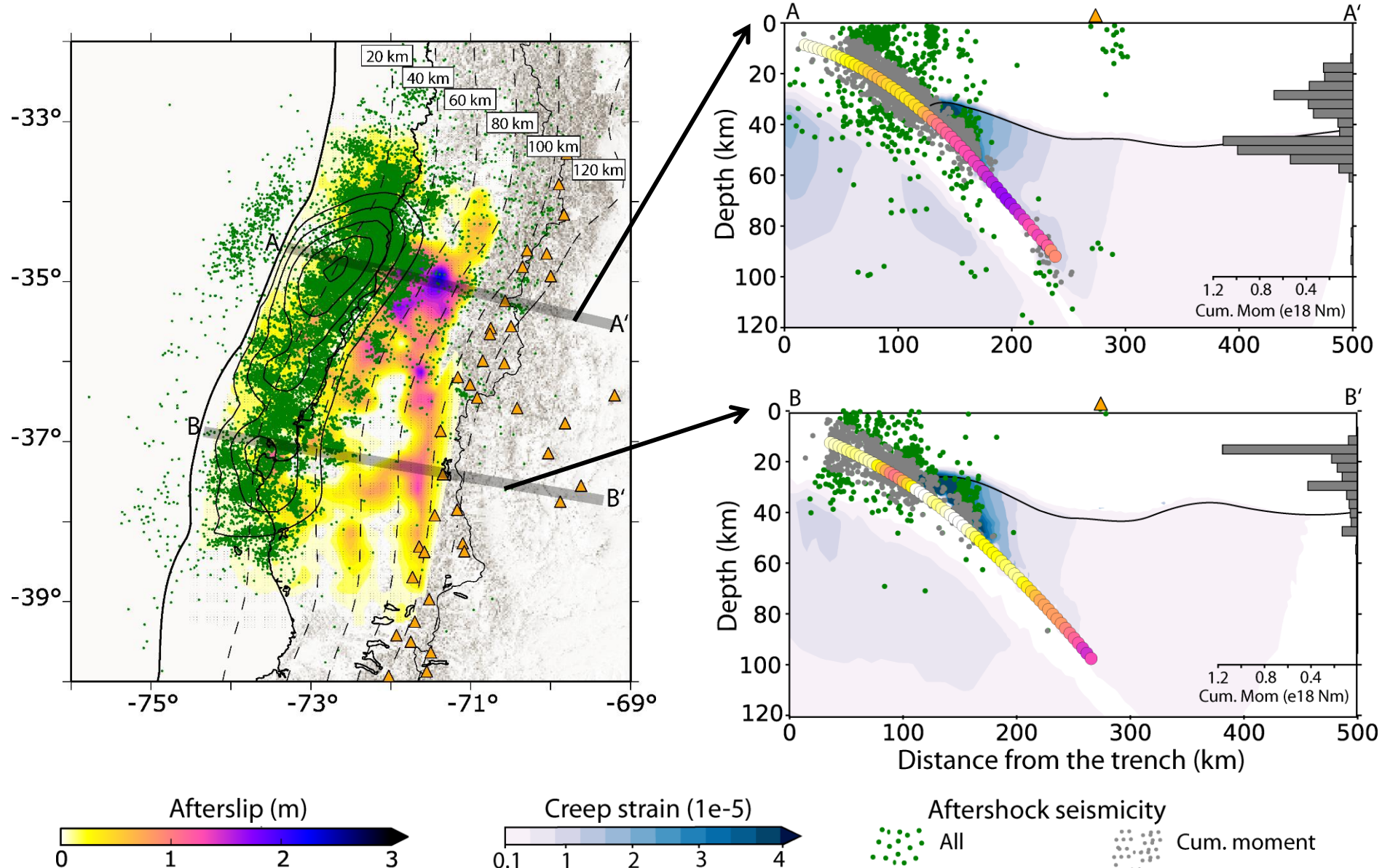
# Afterslip-aftershocks correlation: Power-Law Rheology, Weak Crust



# Afterslip-aftershocks correlation: Power-Law Rheology, Strong Crust

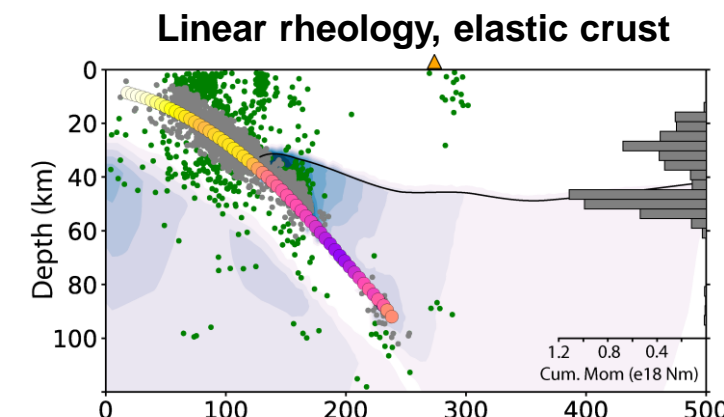
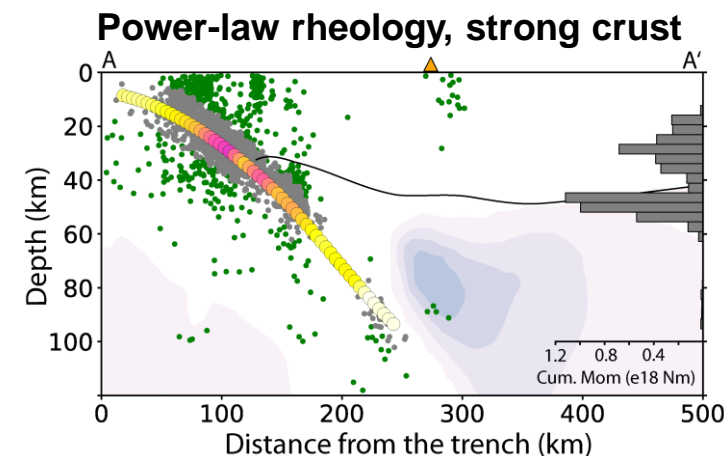
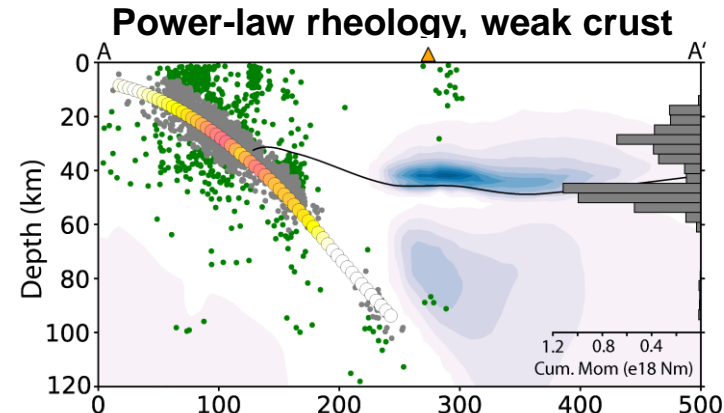


# Afterslip-aftershocks correlation: Linear Rheology, Elastic Crust



# Concluding Remarks

- Inverted deep afterslip and viscoelastic patterns strongly depend on the choice of rheology (linear or power-law), as well as dislocation creep parameters.
- Election of a simulation that also allows non-linear viscoelastic relaxation in the continental lower crust reduces or eliminates the inverted afterslip distribution at the deeper segment (>60 km depth).
- Preferred simulation in the one with weak continental crust because of the best:
  - ✓ Fit to the cumulative GPS displacements.
  - ✓ Fit to the GPS time series.
  - ✓ Spatial correlation between afterslip and aftershock moment release at depths >60 km.



## References

- Agurto-Detzel, H., Font, Y., Charvis, P., Régnier, M., Rietbrock, A., Ambrois, D., Courboulex, F., 2019. Ridge subduction and afterslip control aftershock distribution of the 2016 Mw 7.8 Ecuador earthquake. *Earth Planet. Sci. Lett.* 520, 63–76. <https://doi.org/10.1016/j.epsl.2019.05.029>.
- Avouac, J.-P., 2015. From geodetic imaging of seismic and aseismic fault slip to dynamic modeling of the seismic cycle. *Annu. Rev. Earth Planet. Sci.* 43, 233–271. <https://doi.org/10.1146/annurev-earth-060614-105302>.
- Hayes, G., Wald, D., Johnson, R., 2012. Slab1.0: A three-dimensional model of global subduction zone geometries. *J. Geophys. Res., Solid Earth* 117(B1), B01302. <https://doi.org/10.1029/2011JB008524>.
- Hsu, Y. J., Simons, M., Avouac, J. P., Galetka, J., Sieh, K., Chlieh, M., Natawidjaja, D., Prawirodirdjo, L., Bock, Y., 2006. Frictional afterslip following the 2005 Nias-Simeulue earthquake, Sumatra. *Science* 312 (5782), 1921–1926. <https://doi.org/10.1126/science.1126960>.
- Kato, N., 2007. Expansion of aftershock areas caused by propagating post-seismic sliding. *Geophys. J. Int.* 168(2), 797–808. <https://doi.org/10.1111/j.1365-246X.2006.03255.x>
- Lange, D., Bedford, J., Moreno, M., Tilmann, F., Baez, J., Bevis, M., Krueger, F., 2014. Comparison of postseismic afterslip models with aftershock seismicity for three subduction-zone earthquakes: Nias 2005, Maule 2010 and Tohoku 2011. *Geophys. J. Int.* 199(2), 784–799. <https://doi.org/10.1093/gji/ggu292>.
- Li, S., Moreno, M., Bedford, J., Rosenau, M., Heidbach, O., Melnick, D., and Oncken, O. ( 2017), Postseismic uplift of the Andes following the 2010 Maule earthquake: Implications for mantle rheology, *Geophys. Res. Lett.*, 44, 1768–1776, doi:10.1002/2016GL071995.
- Moreno, M., Melnick, D., Rosenau, M., Baez, J., Klotz, J., Oncken, O., Tassara, A., Chen, J., Bataille, K., Bevis, M., Socquet, A., Bolte, J., Vigny, C., Brooks, B., Ryder, I., Grund, V., Smalley, B., Carrizo, D., Bartsch, M., Hase, H., 2012. Toward understanding tectonic control on the Mw 8.8 2010 Maule Chile earthquake. *Earth Planet. Sci. Lett.* 321–322, 152–165. <https://doi.org/10.1016/j.epsl.2012.01.006>.
- Moreno, M., Rosenau, M., Oncken, O., 2010. 2010 Maule earthquake slip correlates with pre-seismic locking of Andean subduction zone. *Nature* 467(7312), 198–202. <https://doi.org/10.1038/nature09349>.
- Peng, Z., Zhao, P. Migration of early aftershocks following the 2004 Parkfield earthquake. *Nature Geosci* 2, 877–881 (2009). <https://doi.org/10.1038/ngeo697>
- Perfettini, H., Frank, W. B., Marsan, D., & Bouchon, M. ( 2018). A model of aftershock migration driven by afterslip. *Geophysical Research Letters*, 45, 2283–2293. <https://doi.org/10.1002/2017GL076287>
- Perfettini, H., Avouac, J. P., 2007. Modeling afterslip and aftershocks following the 1992 Landers earthquake. *J. Geophys. Res., Solid Earth* 112(B7). <https://doi.org/10.1029/2006JB004399>.
- Peña, C., Heidbach, O., Moreno, M., Bedford, J., Ziegler, M., Tassara, A., Oncken, O., 2020. Impact of power-law rheology on the viscoelastic relaxation pattern and afterslip distribution following the 2010 Mw 8.8 Maule earthquake. *Earth Planet. Sci. Lett.* (In press), <https://doi.org/10.1016/j.epsl.2020.116292>
- Tassara, A., Götze, H. J., Schmidt, S., Hackney, R., 2006. Three-dimensional density model of the Nazca plate and the Andean continental margin. *J. Geophys. Res., Solid Earth* 111(B9). <https://doi.org/10.1029/2005JB003976>.
- Völker, D., Grevemeyer, I., Stipp, M., Wang, K. He, J., 2011. Thermal control of the seismogenic zone of southern central Chile. *J. Geophys. Res.* 116(B10). <https://doi.org/10.1029/2011JB008247>.
- Wang, K., Hu, Y., He, J., 2012. Deformation cycles of subduction earthquakes in a viscoelastic Earth, *Nature* 484(7394), 327–332. <https://doi.org/10.1038/nature11032>.